Quantification of branching in model 3-arm star polyethylene

Ramnath Ramachandran, Gregory Beaucage* and Durgesh K Rai
Department of Chemical and Materials Engineering, University of Cincinnati, Cincinnati, Ohio 45221, USA

David J. Lohse, Thomas Sun, Andy H. Tsou and Alexander Norman
Corporate Strategic Research Labs, ExxonMobil Research & Engineering Co., Annandale, New Jersey 08801, USA

Nikos Hadjichristidis
Department of Chemistry, University of Athens, Panepistimiopolis, Zografou, 157 84 Athens, Greece

Abstract

The versatility of a novel scaling approach in quantifying the structure of model well-defined 3-arm star polyethylene molecules is presented. Many commercial polyethylenes have long side branches, and the nature and quantity of these branches varies widely among the various forms. For instance, low-density polyethylene (LDPE) is typically a highly branched structure with broad distributions in branch content, branch lengths and branch generation (in hyperbranched structures). This makes it difficult to accurately quantify the structure and the inherent structure-property relationships. To overcome this drawback, model well-defined hydrogenated polybutadiene (HPB) structures have been synthesized via anionic polymerization to serve as model analogs to long-chain branched polyethylene. In this article, model 3-arm star polyethylene molecules are quantified using the scaling approach. Along with the long-chain branch content in polyethylene, the approach also provides unique measurements of long-chain branch length and hyperbranch content. Such detailed description facilitates better understanding of the effect of branching on the physical properties of polyethylene.

* Corresponding author

Introduction

The molecular structure of commercial polyethylenes varies widely among the several forms that have proven useful in the marketplace. In particular, the levels and types of long chain branching vary greatly. One finds nearly linear structures to low levels of long-chain branching in linear-low density polyethylene (LLDPE) and high density polyethylene (HDPE). Higher levels of long-chain branching is seen in low density polyethylene (LDPE). Long-chain branching in polyethylene is known to have significant effects on its chain dimensions and physical properties.[1-3] For instance, the presence of long-chain branches in low-density polyethylene (LDPE) significantly improves its processability. In order to quantify the branch content in polyethylene, techniques such as gel permeation chromatography (GPC), nuclear magnetic resonance (NMR) spectroscopy, light scattering, and rheological measurements are frequently employed. Essentially, these techniques measure the number-average long-chain branches per chain, which is not sufficient to provide a detailed description of the structure of polyethylene.[4-6] Moreover, the limitations of these techniques lead to incomprehensive quantification of branching. For instance while GPC is ineffective in measuring low levels of branching,[4] NMR is unable to distinguish between branches exceeding six carbon atoms in length.[7] A novel scaling approach has been developed recently to quantify the branch content in ramified structures such as polyethylene.[8] The scaling model,[4, 8] when applied to small-angle neutron scattering (SANS) data, can quantify both short-chain branching[9] and long-chain branching in polyethylene.[5] The scaling approach has been used previously to characterize other ramified materials such as ceramic aggregates,[8] proteins,[10] hyper-branched polymers[11] and cyclic polymers.[12]

LDPE is an industrially important polyethylene and typically displays broad distributions in molecular weight, branch content and branch length. Hence it is difficult to get an accurate quantification of the nature of the long-chain branching and its effect on physical properties. To better understand the structure-property relationships due to the presence of long-chain branches, it is desirable to have model structures with a low polydispersity index as well as controlled levels of branch content and branch length. Anionic polymerization is one of the most useful techniques in synthesizing polymers having precisely controlled structures.[13-15] This form of living polymerization is characterized by its rapid initiation step and elimination of chain transfer and termination reactions that results in nearly monodisperse polymers. While it is not possible to synthesize polyethylene directly by this technique, it is possible to synthesize model polybutadiene that can be hydrogenated to eliminate unsaturation and form analogs of polyethylene.[1, 16] Polybutadiene synthesized by anionic polymerization have cis, trans and vinyl double bonds incorporated in the structure. Upon hydrogenation, the cis and trans double bonds are removed while the vinyl double bonds result in ethyl short-chain branches.[14] Long-chain branched polybutadiene can be prepared using chlorosilane condensation chemistry. [1, 16, 17] Hadjichristidis *et al.* have synthesized[1] a variety of model branched polyethylene analogs by hydrogenating branched polybutadienes. These include polyethylene with 3-arm star, comb, H and pom-pom architectures. In this article, the aforementioned scaling approach[4, 5, 8] is applied to quantify the structure of model 3-arm star polyethylene synthesized by Hadjichristidis *et al*.[1] The versatility of the scaling approach is highlighted here by presenting the detailed quantification of such model branched polyethylene resins.

Scaling Model

Polyolefins like polyethylene (PE) in dilute solution display two structural levels: the average chain size R with mass-fractal dimension d_f and an average substructural rod-like persistence unit of length l_p[†] or Kuhn length $l_k \approx 2l_p$.[18] These structural levels are observed in small-angle scattering patterns from polyethylene. The Unified Function[5, 6, 8, 9, 19, 20] used in this article is useful in quantifying these structural levels in terms of their size and associated mass-fractal dimensions. A branched polymer like polyethylene can be described in terms of two distinct features. One is a short circuit path through the branched structure that displays an average tortuosity linked to the thermodynamic conditions and steric constraints. The other is an average connectivity based on the branch content, which is invariant to changes in thermodynamic conditions. These two average features of branched polymers can be described using a universal scaling model.[8] The scaling model has been used previously in describing the structure and quantifying the topology of a variety of mass-fractals.[4, 5, 8-12]

Considering a polyethylene chain of end-to-end distance R and mass-fractal dimension d_f composed of z Kuhn steps of size l_k (see Figure 1), the scaling model describes an average short-circuit path or minimum path p with mass-fractal dimension d_{min}. The tortuosity in the polyethylene chain is described by p and d_{min}. The connectivity of the polyethylene chain can be described by a connecting path s with an associated connectivity dimension, c, that is obtained by joining chain ends and branch points with straight lines. z, p and s can be related to the chain size R/l_k by,

[†] Additionally, a dynamic size close to l_p called the packing length [3] can be defined which is not discussed here.

$$z = \left(\frac{R}{l_k}\right)^{d_f}, p = \left(\frac{R}{l_k}\right)^{d_{\min}} \; and \;\; s = \left(\frac{R}{l_k}\right)^{c} \tag{1}$$

A scaling relationship between z, p and s can then be derived as,[5, 8]

$$z = p^{c} = s^{d_{\min}} \tag{2}$$

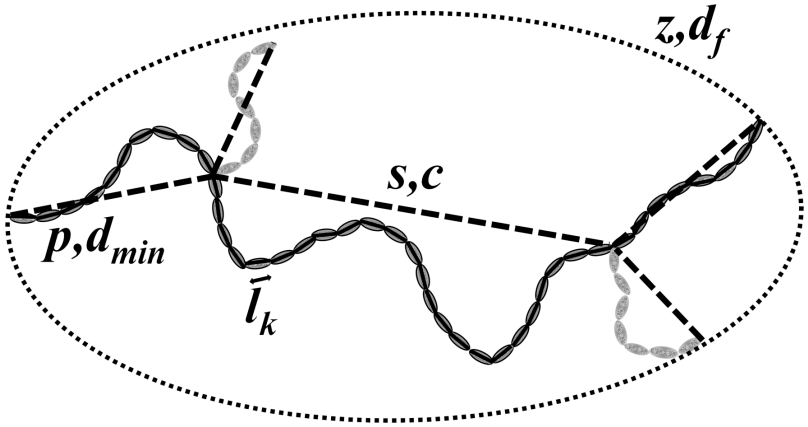

Figure 1. Schematic of a branched polymer in the scaling model. Each Kuhn step is represented by a bead. The polymer of mass-fractal dimension d_f is composed of z Kuhn steps of size l_k. The dark beads represent a minimum path p of dimension d_{min}. The lighter Kuhn steps symbolize the long-chain branches. The dotted lines represent the connective path of length s and dimension c.

From Eqs. 1 and 2 a simple relationship is obtained, $d_f = cd_{min}$, that shows how chain scaling is described via contributions from tortuosity and connectivity. For regular objects like rods and discs that are completely connected and have no tortuosity through the structure, $d_f = c$ and $d_{min} = 1$. d_{min} increases with tortuosity, c increases with increased connectivity. Thus for linear polyethylene in a good solvent, $d_f = d_{min} \approx 5/3$ and $c = 1$. For branched polyethylene in a good solvent, $d_f > d_{min}$, $1 < c \leq d_f$ and $1 \leq d_{min} \leq 5/3$.

In the scaling approach,[4-6, 8] to describe a branched polymer chain of molecular weight z, we define a minimum path, p, which is the molecular weight of the short-circuit path taken through the polymer chain from one end to another. The part of the molecule outside of the minimum path, z-p, is then considered to be as branches. Thereby, the mole fraction long-chain branch content, ϕ_{br}, is obtained by,

$$\phi_{br} = \frac{z-p}{z} = 1 - z^{\frac{1}{c}-1} \tag{3}$$

The calculation of branch fraction for symmetric stars is trivial and can be calculated by[8], $\phi_{br} = \frac{f-2}{f}$, where f is the functionality of the symmetric star. For asymmetric stars, 3 different minimum paths (short circuits) are possible through the structure. The average minimum path can then be calculated as a weight-average moment of this path. For the model star polyethylene in this paper, where information about number of arms and arm lengths is available (see Table 2), an expression to obtain weight-average branch content is given by,

$$\phi_{br,wt-avg} = \frac{\sum_{i=1}^{3}(z-p_i)^2 \Big/ \sum_{i=1}^{3}(z-p_i)}{z} \tag{3a}$$

The Unified Function[5, 9, 19, 20] along with the scaling model[8] when applied to scattering data from polyethylene provides substantial information to describe the topology of branched polyethylene. For example, the Unified Function in Eq. 4 gives R_{g2}, G_2, B_2, G_1, B_1 and d_f.

$$I(q) = \left\{ G_2 e^{-\left(q^2 R_{g2}^2\right)/3} + B_2 e^{-\left(q^2 R_{g1}^2\right)/3} \left(q_2^*\right)^{-d_{f2}} \right\} + \left\{ G_1 e^{-\left(q^2 R_{g1}^2\right)/3} + B_1 \left(q_1^*\right)^{-1} \right\} \tag{4}$$

where $q_i^* = \left[\frac{q}{\left\{ erf\left(qkR_{gi}/\sqrt{6}\right) \right\}^3} \right]$ and $k \approx 1.06$

The terms in the first bracket with subscript "2" represent the overall chain size and the second bracket with subscript "1" represent the rod-like persistent scaling regime. The minimum dimension, d_{min}, is calculated from these parameters and is given by,[5, 8]

$$d_{\min} = \frac{B_2 R_{g,2}^{d_f}}{C_p \Gamma\left(\frac{d_f}{2}\right) G_2} \tag{5}$$

where C_p is the polydispersity factor[5, 9, 21] and Γ is the gamma function. The weight-average number of Kuhn steps, z, is given by the ratio of G_2 over G_1.[8, 9, 20] The connectivity dimension, c, is obtained from d_f/d_{min} as described in the scaling model. From the topological parameters obtained, an expression is derived[5] for the weight-average number of branch sites per chain, n_{br}, which is given by,[5]

$$n_{br} = \left(\frac{z^{\left(\frac{5}{2}d_f - \frac{3}{2}c\right) + \left(1 - \frac{1}{c}\right)} - 1}{2} \right) \tag{6}$$

The weight-average n_{br} is comparable to the number of long-chain branches per chain that is obtained from NMR[5, 22] for tri-functional branch points except that the NMR measurement is a number-average. The weight-average long-chain branch length, z_{br}, is determined by,

$$z_{br} = \frac{z\phi_{br}M_{Kuhn}}{n_{br,p}} \tag{7}$$

where M_{Kuhn} is the mass of one Kuhn step and assuming $f = 3$ (branch site functionality). For polyethylene, $M_{Kuhn} = 13.4\ l_k$, where M_{Kuhn} has units of g/mole and l_k has units of Å.[5] $n_{br,p}$ represents the average number of branches per minimum path. Using n_{br} and $n_{br,p,}$ an expression for the hyperbranch content in terms of the average number of inner segments per chain, $n_i = n_{br} - n_{br,p}$ is obtained.[5] Inner segments refer to segments in a polymer that have branch points at both ends.

Materials and Methods

Well-controlled model 3-arm star polyethylene resins analyzed in this article were derived by saturation of anionically synthesized polydienes.[1, 16] The resins included both symmetric (A_3 type) and asymmetric 3-arm (A_2B) stars, where A and B represent the individual arms in the 3-arm star polyethylene. A detailed description of the synthesis of the polybutadiene precursors and the subsequent hydrogenation to obtain the polyethylene analogs are given elsewhere.[1] These model polymers have been well studied and characterized in the literature.[1, 2] SANS was performed on dilute solutions of model 3-arm star hydrogenated polybutadiene in deuterated p-xylene which is a good solvent for polyethylene at 125° C. 500 ppm of

butylhydroxytoluene (BHT) was used as a stabilizer and dissolved in the solvent during sample preparation. BHT and deuterated p-xylene were purchased from Fisher Scientific. The samples were equilibrated at 125 °C for 2 hours prior to the measurements to ensure complete dissolution of the polymer. The polymer solution was stirred by means of micro-magnetic stir bars to homogenize the solution prior to the measurement. 1 wt. % solutions were used which is well below the overlap concentration [23] for all fractions. SANS experiments were carried out at NG-7 SANS [24] at the National Institute of Standards and Technology (NIST) Center for Neutron Research (NCNR), Gaithersburg. Standard data correction procedures for transmission and incoherent scattering along with secondary standards were used to obtain $I(q)$ vs. q in absolute units [25]. Experimental runs took approximately 2 hours per sample.

Results and Discussions

The corrected SANS data for the 3-arm star polyethylene were plotted in log-log plots of $I(q)$ vs. q and fit to the Unified Function in Eq. 4 followed by the application of the scaling model. Table 1 lists the sample names along with weight-average molecular weight and polydispersity index, PDI, measured from SEC-MALLS.[1] Table 1 also lists the quantities estimated from SANS and the scaling model that include weight-average molecular weight, mole-fraction long-chain branch content, ϕ_{br}, from Eq. 3, number of long-chain branch sites per chain, n_{br}, from Eq. 6, average long-chain branch length, z_{br}, from Eq. 7 and number of inner segments per chain, n_{i}, that was estimated as described in reference [5]. n_{i} is a measure of the hyperbranch content in a polymer chain.[5] The last column in Table 1 lists the measured steric

interaction in the 3-arm star polymers, ϕ_{si}, which is described later in this article. The errors reported were propagated from the data.

Table 1: SANS characterization of model 3-arm star polyethylene resins

Sample	M_w (kg/mol)[a]	PDI (M_w/M_n)[a]	M_w (kg/mol)[b]	ϕ_{br}	n_{br}	z_{br} (kg/mol)	n_i	ϕ_{si}
$PES(50)_2(5)$	130	1.03	135±10	0.42±0.02	1.21±0.05	47±5	0.23±0.09	0.033±0.005
$PES(50)_2(15)$	138	1.04	135±8	0.40±0.02	0.93±0.04	54±5	0.22±0.08	0.026±0.005
$PES(50)_2(25)$	131	1.06	134±9	0.42±0.02	0.97±0.04	49±5	0.26±0.08	0.027±0.005
$PES(43)_3$	133	1.13	135±9	0.34±0.01	0.76±0.03	44±4	0.10±0.05	0.026±0.006
$PES(15)_2(85)$	129	1.17	128±13	0.61±0.03	1.88±0.07	66±6	1.00±0.12	0.034±0.005
$PES(40)_2(60)$	125	1.08	137±8	0.39±0.03	0.87±0.06	59±7	0.20±0.10	0.024±0.004
$PES(27)_3$	82	1.04	103±5	0.36±0.02	0.90±0.06	33±4	0.10±0.08	0.032±0.005
$PES(53)_3$	139	1.12	132±7	0.34±0.02	0.81±0.05	49±6	0.08±0.06	0.025±0.005
$PES(48)_3$	138	1.21	146±7	0.35±0.01	0.80±0.06	51±4	0.11±0.08	0.024±0.004

[a]measured by SEC-MALLS
[b]measured by SANS.

Scattering techniques like light, x-ray and neutron scattering measure the weight-average molecular weight, M_w, of polymers. In this paper, a number of quantities including M_w are measured from SANS. The analysis of model 3-arm star polyethylene can allow us to verify if these quantities are weight-average. The molecular weight of 3-arm star polyethylene resins were estimated from SANS using a method described by Boothroyd *et.al*.[26] Figure 2 plots the weight-average molecular weight, M_w, obtained from SANS against weight-average molecular weight, M_w, from SEC-MALLS.[1] The data shows reasonable agreement between the molecular weight measured from the two techniques (error bars are not available for SEC-MALLS values).

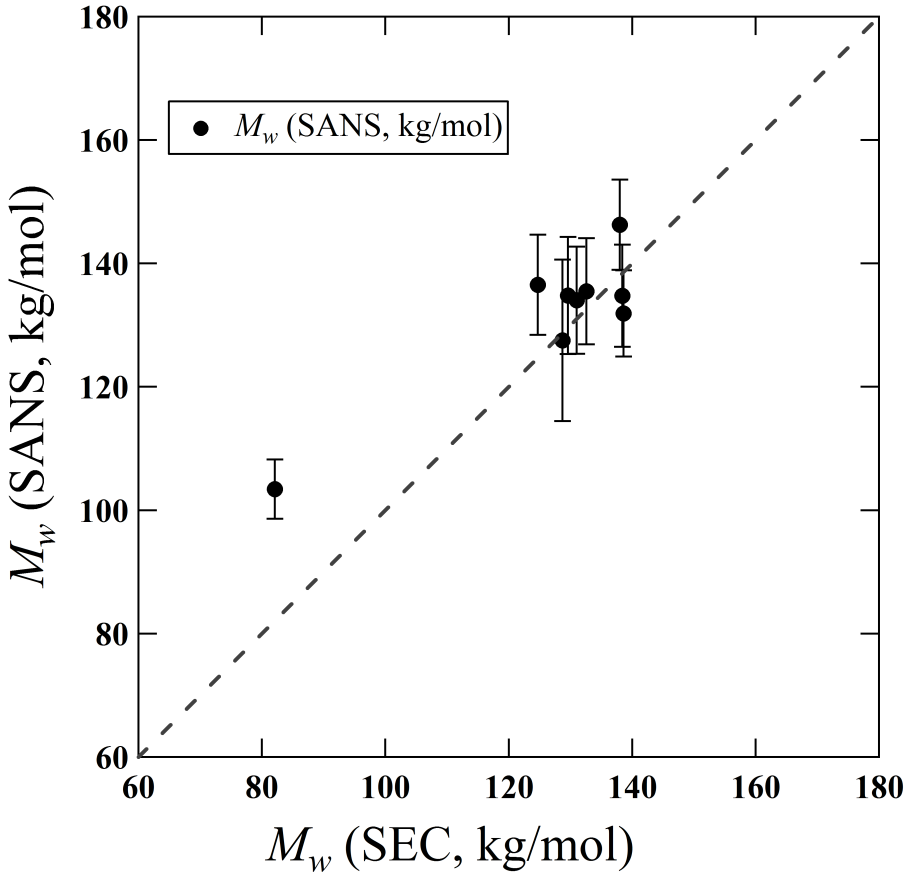

Figure 2. Plot of weight-average molecular weight, M_w, obtained from SANS and weight-average molecular weight, M_w, obtained from SEC-MALLS.

Figure 3 plots the mole-fraction branch content, ϕ_{br}, from Eq. 3, obtained from SANS against $\phi_{br,wt-avg}$ obtained from Eq. 3a. In a previous study[6] conducted on commercial linear low-density polyethylene fractions, mole-fraction branch content measured for the parent resin using the SANS-scaling approach was found to be in good agreement with corresponding weight-average values calculated by summing the contribution from individual fractions. In the current study, the good correlation between ϕ_{br} and $\phi_{br,wt-avg}$ seen in Figure 3 for the model long-chain

branched polyethylene is compelling evidence that the branch fraction measured from the SANS-scaling approach is a weight-average quantity.

Using the individual arm-lengths available in Table 2, it is possible to calculate the weight-average arm length, $z_{br,wt\text{-}avg}$, for the model 3-arm star resins by,

$$z_{br,wt-avg} = \frac{\sum_{i=1}^{3} (Arm)_i^2}{\sum_{i=1}^{3} (Arm)_i} \tag{8}$$

Figure 4 plots the average branch length, z_{br}, from Eq. 7, obtained from SANS versus weight-average arm length, $z_{br,wt\text{-}avg}$, from Eq. 8. The good correlation seen in figure 4 substantiates that the average branch length measured from the SANS-scaling approach is a weight-average quantity.

Table 2. Arm lengths for 3-arm star polyethylene

Sample	Arm 1 (kg/mol)	Arm 2 (kg/mol)	Arm 3 (kg/mol)	$z_{br,wt\text{-}avg}$ (kg/mol)
$PES(50)_2(5)$	52	52	5.2	49.8
$PES(50)_2(15)$	52	52	15.5	47.3
$PES(50)_2(25)$	52	52	26	46.8
$PES(43)_3$	44.5	44.5	44.5	44.5
$PES(15)_2(85)$	15.5	15.5	88.5	69.6
$PES(40)_2(60)$	42	42	62	50.5
$PES(27)_3$	28	28	28	28
$PES(53)_3$	55	55	55	55
$PES(48)_3$	48	48	48	48

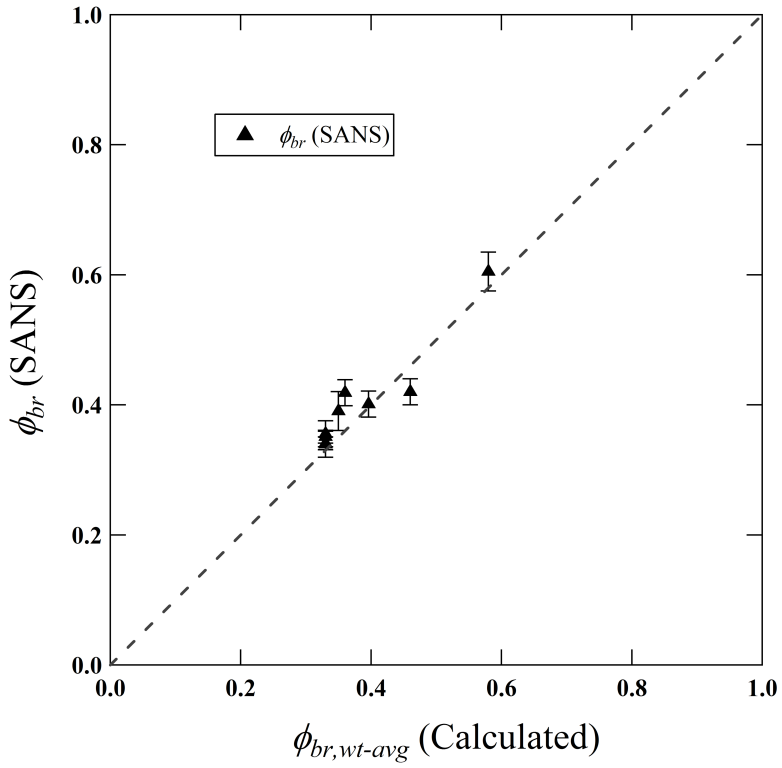

Figure 3. Plot of mole-fraction branch content, ϕ_{br}, from Eq. 3, obtained from SANS versus the calculated weight-average branch content, $\phi_{br,wt-avg}$, from Eq. 3a.

The SANS-scaling approach uniquely quantifies the average hyperbranch content in terms of the average number of inner segments, n_i, in a hyperbranched polymer. Previously it was seen that n_i has significant impact on rheological properties such as the zero-shear rate viscosity enhancement in branched polyethylene.[5] Table 3 lists the zero-shear rate viscosity and the zero-shear rate viscosity enhancement for certain 3-arm star polyethylenes where data was available in the literature.[2] A linear polyethylene with similar weight-average molecular weight was chosen to determine the enhancement for the branched polymers. Figure 5 plots the hyperbranch content, n_i, measured from SANS versus the zero-shear rate viscosity enhancement,

$\eta_0/\eta_{0,L}$. Almost all the resins show very low hyperbranch content and it can be concluded that the viscosity enhancement is primarily due to the presence of a branch. In the case of PES(15)$_2$(85), it is seen that the viscosity enhancement is much higher when compared to the other resins. Correspondingly, high hyperbranch content is also measured for this resin. While it is not expected that hydrogenated 3-arm star polybutadienes prepared using chlorosilane condensation chemistry[1] have any hyperbranching, the distinctively high viscosity enhancement (along with a measured n_{br} = 1.88 ± 0.07) for PES(15)$_2$(85) seems to indicate the presence of an additional hyperbranched arm (leading to an inner segment) in this resin. Additionally, considering the measured average branch length, z_{br}, for PES(15)$_2$(85), it can be inferred that the additional arm is the smaller arm (15.5 kg/mole) of the asymmetric star. It is also possible that the higher polydispersity index (see Table 1) for this resin is an artifact of this hyperbranching.

The data plotted in Figure 5 can be treated analogous to Figure 4b in Reference 9. We can consider the polyethylene melt as a dilute solution of hyperbranched segments in a melt of non-hyperbranched 3-arm star polyethylene. A linear functionality of $\eta_0/\eta_{0,L}$ in n_i is then analogous to a dilute suspension of particulates. The Einstein equation[32] for a dilute particulate suspension, $\eta_0=\eta_{0,L}(1+n_i[\eta_0])$, can be used as an approximation, except that there is a shift of 0.1on the n_i axis. We obtain a slope of 7550 chains/inner segment corresponding to a type of intrinsic viscosity for hyperbranched structures in a suspension of non-hyperbranched chains. This slope is much higher than the 278 chains/inner segment observed previously for certain metallocene polyethylene.[9] The higher slope can be explained due to the presence of the hyperbranched segments among pure branched 3-arm star chains rather than mostly linear chain as in the case of

the metallocene polyethylene.[9] The 3-arm stars dynamically interact to a greater extent than their linear analogues thereby amplifying the effect of inner segments.

Table 3. Zero-shear rate viscosity enhancement for 3-arm star polyethylene[a]

Sample	η_0 (Pa.S)	$\eta_0/\eta_{0,L}$
$PES(50)_2(5)$	9.25×10^5	141
$PES(50)_2(15)$	8.56×10^6	1300
$PES(50)_2(25)$	2.28×10^6	347
$PES(43)_3$	5.70×10^6	866
$PES(15)_2(85)$	4.60×10^7	6990
$PES(40)_2(60)$	6.42×10^6	976

[a]From reference 2

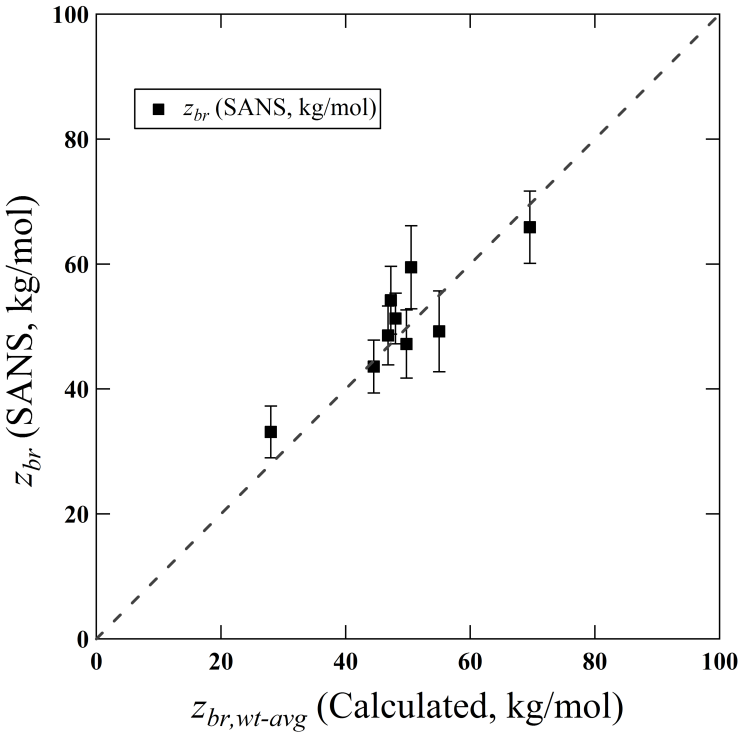

Figure 4. Plot of average branch length, z_{br}, obtained from SANS using Eq. 7 versus the calculated weight-average arm length, $z_{br,wt\text{-}avg}$, from Eq. 8 for 3-arm star polyethylene.

For star polymers in general, the presence of arms can lead to steric interactions between arms. Such steric effects are expected to be the lowest for 3-arm stars and increase with higher number of arms. In the scaling approach, for a linear polymer chain in a good solvent, $d_{\min} = 5/3$. For a theoretical star polymer with a large number of arms, the steric interaction will be at a maximum. At such a state, the polymer chains could be fully extended (rod like) with $d_{\min}=1$. Using the limits of a linear chain and infinite-arm star, an expression can be obtained to quantify the steric interaction factor in a star polymer, ϕ_{si}, that is given by,

$$\phi_{si} = \frac{s_{observed} - s_{unperturbed}}{s_{extended} - s_{unperturbed}} = \frac{z^{1/d_{\min}} - z^{3/5}}{z^{1} - z^{3/5}} \qquad (10)$$

Table 1 lists the ϕ_{si} measured for the 3-arm star polymers analyzed in this article. As expected, the steric interaction is very low for these polymers. For the symmetric 3-arm star polymers, while the measured ϕ_{si} values do not show much variation, the data seems to suggest that the steric interaction increases with increasing average number of arms per chain, n_{br} (see Table 1). Additionally, figure 6 shows a possible dependence of the steric interaction factor on the geometric mean arm length. In a forthcoming paper, a series of multi-arm star polymers will be treated with the scaling approach in order to determine the relationship between the number of arms, arm length and steric interaction factor in star polymers.

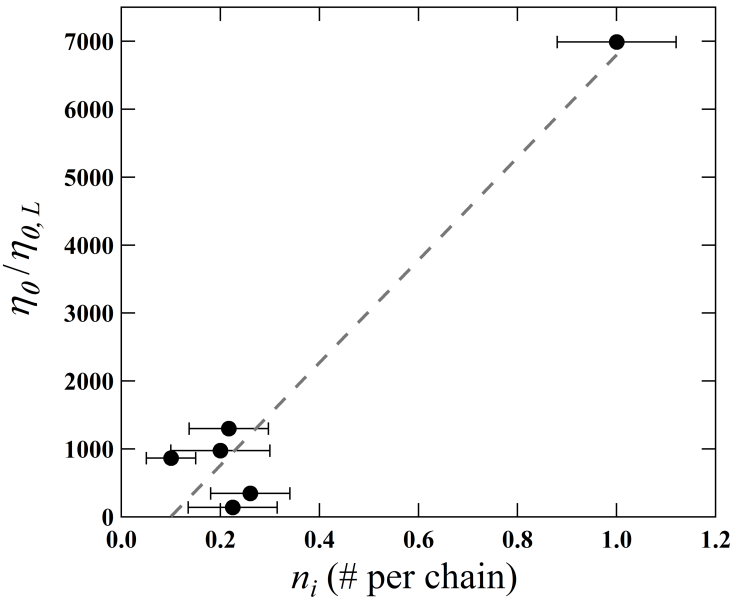

Figure 5. Plot of the zero-shear rate viscosity enhancement, $\eta_0/\ \eta_{0,L}$, versus the hyperbranch content, n_i, measured from SANS.

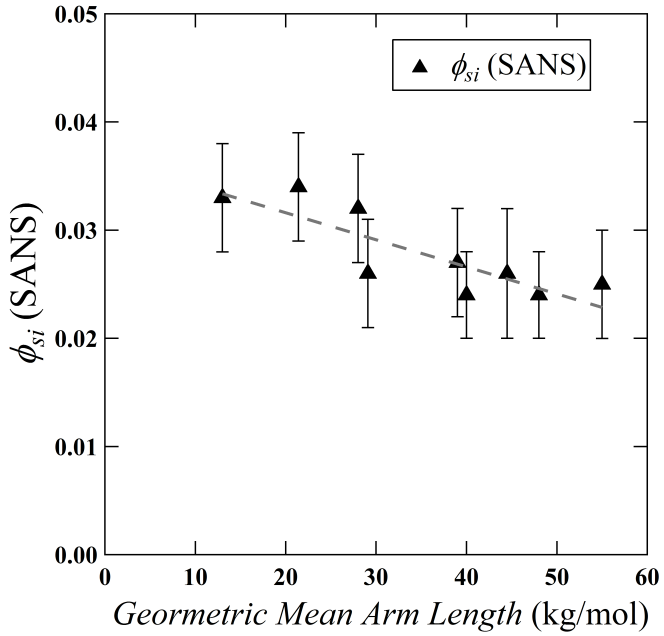

Figure 6. Plot of the steric interaction factor, ϕ_{si}, versus the calculated geometric mean arm length. Dotted line is a trend line.

Conclusion

A novel scaling approach to quantify the topology of complex structures has been presented in this article. The usefulness of the scaling approach in quantifying the branch content of model polyethylene resins was illustrated. Along with estimating the average number of long-chain branches per polymer chain, n_{br}, the approach provides unique measurements of mole-fraction branch content, ϕ_{br}, average long-chain branch length, z_{br}, hyperbranch content, n_{i}, and steric interaction due to branching, ϕ_{si}. The measurements of ϕ_{br} and z_{br} made via the SANS-scaling approach show good correlation with the calculated averages for these model 3-arm star resins. Additionally, the high viscosity enhancement in a particular 3-arm star resin was attributed to the presence of hyperbranched segments that was measured using the SANS-scaling approach. The example discussed in this article demonstrates how the detailed quantification available using the scaling approach can lead to better understanding of the effects of polymer structure on physical properties. The scaling approach can also be employed to quantify branching in other complex structures such as ceramic aggregates[8], cyclic polymers[13] and to quantify the degree of folding in proteins and RNA.[11]

Acknowledgements

This work was funded by ExxonMobil Research & Engineering Co. and the University of Cincinnati Graduate School Distinguished Dissertation Completion Fellowship. This work utilized facilities supported in part by the National Science Foundation under Agreement No. DMR-0454672. We acknowledge the support of the National Institute of Standards and Technology (NIST), U.S. Department of Commerce, for providing the neutron research facilities

used in this work. Research at Oak Ridge National Laboratory's High Flux Isotope Reactor was sponsored by the Scientific User Facilities Division, Office of Basic Energy Sciences, U.S. Department of Energy. We thank B. Hammouda and S. Kline at NIST and Y. Melnichenko at ORNL for their valuable support during the beamtime.

References

1. Hadjichristidis, N.; Xenidou, M.; Iatrou, H.; Pitsikalis, M.; Poulos, Y.; Avgeropoulos, A.; Sioula, S.; Paraskeva, S.; Velis, G.; Lohse, D. J.; Schulz, D. N.; Fetters, L. J.; Wright, P. J.; Mendelson, R. A.; Garcia-Franco, C. A.; Sun, T.; Ruff, C. J. *Macromolecules* **2000,** 33, (7), 2424-2436.

2. Lohse, D. J.; Milner, S. T.; Fetters, L. J.; Xenidou, M.; Hadjichristidis, N.; Mendelson, R. A.; Garcia-Franco, C. A.; Lyon, M. K. *Macromolecules* **2002,** 35, (8), 3066-3075.

3. Garcia-Franco, C. A.; Harrington, B. A.; Lohse, D. J. *Macromolecules* **2006,** 39, (7), 2710-2717.

4. Kulkarni, A. S.; Beaucage, G. *Journal of Polymer Science Part B-Polymer Physics* **2006,** 44, (10), 1395-1405.

5. Ramachandran, R.; Beaucage, G.; Kulkarni, A. S.; McFaddin, D.; Merrick-Mack, J.; Galiatsatos, V. *Macromolecules* **2009,** 42, (13), 4746-4750.

6. Ramachandran, R.; Beaucage, G.; McFaddin, D.; Merrick-Mack, J.; Galiatsatos, V.; Mirabella, F. *Polymer* **2011,** 52, (12), 2661-2666.

7. Bovey, F. A. *Pure and Applied Chemistry* **1982,** 54, (3), 559-568.

8. Beaucage, G. *Physical Review E* **2004,** 70, (3).

9. Ramachandran, R.; Beaucage, G.; Kulkarni, A. S.; McFaddin, D.; Merrick-Mack, J.; Galiatsatos, V. *Macromolecules* **2008,** 41, (24), 9802-9806.

10. Beaucage, G. *Biophysical Journal* **2008,** 95, (2), 503-509.

11. Kulkarni, A. S.; Beaucage, G. *Macromolecular Rapid Communications* **2007,** 28, (12), 1312-1316.

12. Beaucage, G.; Kulkarni, A. S. *Macromolecules* **2010,** 43, (1), 532-537.

13. Hsieh, H. L.; Quirk, R. P., *Anionic polymerization: Principles and Practical Application*. Marcel Dekker: New York, 1996.

14. Morton, M., *Anionic Polymerization: Principles and Practice*. Academic Press: New York, 1983.

15. Hadjichristidis, N.; Iatrou, H.; Pispas, S.; Pitsikalis, M. *Journal of Polymer Science Part a-Polymer Chemistry* **2000,** 38, (18), 3211-3234.

16. Rachapudy, H.; Smith, G. G.; Raju, V. R.; Graessley, W. W. *Journal of Polymer Science Part B-Polymer Physics* **1979,** 17, (7), 1211-1222.

17. Rochefort, W. E.; Smith, G. G.; Rachapudy, H.; Raju, V. R.; Graessley, W. W. *Journal of Polymer Science Part B-Polymer Physics* **1979,** 17, (7), 1197-1210.

18. Doi, M.; See, H., *Introduction to polymer physics*. Clarendon Press: 1996.

19. Beaucage, G. *Journal of Applied Crystallography* **1995,** 28, 717-728.

20. Beaucage, G. *Journal of Applied Crystallography* **1996,** 29, 134-146.

21. Sorensen, C. M.; Wang, G. M. *Physical Review E* **1999,** 60, (6), 7143-7148.

22. Costeux, S.; Wood-Adams, P.; Beigzadeh, D. *Macromolecules* **2002,** 35, (7), 2514-2528.

23. Murase, H.; Kume, T.; Hashimoto, T.; Ohta, Y.; Mizukami, T. *Macromolecules* **1995,** 28, (23), 7724-7729.

24. Glinka, C. J.; Barker, J. G.; Hammouda, B.; Krueger, S.; Moyer, J. J.; Orts, W. J. *Journal of Applied Crystallography* **1998,** 31, 430-445.

25. Kline, S. R. *Journal of Applied Crystallography* **2006,** 39, 895-900.

26. Boothroyd, A. T.; Squires, G. L.; Fetters, L. J.; Rennie, A. R.; Horton, J. C.; Devallera, A. *Macromolecules* **1989,** 22, (7), 3130-3137.